SPE-208125-MS

A Critical Literature Review on Rock Petrophysical Properties Estimation from Images Based on Direct Simulation and Machine Learning Techniques

Ahmed Samir Rizk, Moussa Tembely, Waleed AlAmeri, and Emad W. Al-Shalabi, Khalifa University of Science and Technology

This paper was prepared for presentation at the Abu Dhabi International Petroleum Exhibition & Conference to be held in Abu Dhabi, UAE, 15 – 18 November 2021. The official proceedings were published online on 9 December 2021.

Abstract

Estimation of petrophysical properties is essential for accurate reservoir predictions. In recent years, extensive work has been dedicated into training different machine-learning (ML) models to predict petrophysical properties of digital rock using dry rock images along with data from single-phase direct simulations, such as lattice Boltzmann method (LBM) and finite volume method (FVM). The objective of this paper is to present a comprehensive literature review on petrophysical properties estimation from dry rock images using different ML workflows and direct simulation methods. The review provides detailed comparison between different ML algorithms that have been used in the literature to estimate porosity, permeability, tortuosity, and effective diffusivity. In this paper, various ML workflows from the literature are screened and compared in terms of the training data set, the testing data set, the extracted features, the algorithms employed as well as their accuracy. A thorough description of the most commonly used algorithms is also provided to better understand the functionality of these algorithms to encode the relationship between the rock images and their respective petrophysical properties.

The review of various ML workflows for estimating rock petrophysical properties from dry images shows that models trained using features extracted from the image (physics-informed models) outperformed models trained on the dry images directly. In addition, certain tree-based ML algorithms, such as random forest, gradient boosting, and extreme gradient boosting can produce accurate predictions that are comparable to deep learning algorithms such as deep neural networks (DNNs) and convolutional neural networks (CNNs). To the best of our knowledge, this is the first work dedicated to exploring and comparing between different ML frameworks that have recently been used to accurately and efficiently estimate rock petrophysical properties from images. This work will enable other researchers to have a broad understanding about the topic and help in developing new ML workflows or further modifying exiting ones in order to improve the characterization of rock properties. Also, this comparison represents a guide to understand the performance and applicability of different ML algorithms. Moreover, the review helps the researchers in this area to cope with digital innovations in porous media characterization in this fourth industrial age – oil and gas 4.0.

Introduction and Background

Several techniques have been developed to estimate porosity, permeability, and other rock petrophysical properties. One of these extensively used methods is laboratory measurements through routine core analysis. Nevertheless, experiments can be costly, destructive, and time-consuming to perform as well as the respective measurements can be constrained to specific operating conditions (Andrä *et al.*, 2013a; Blunt *et al.*, 2013; Santos *et al.*, 2020,). In addition, rock properties can be estimated using empirical correlations (Van der Linden *et al.*, 2016; Wu *et al.*, 2019).

Direct pore-scale simulation, as an alternative approach, has been widely used recently to obtain different single phase and multiphase flow properties from digital rock images. Direct simulation methods emerged as an attractive complement or even potential replacement for laboratory measurements, particularly with the increasing capability of X-ray scanners and high-performance computing clusters (Keehm, 2003; Meng *et al.*, 2008; Andrä *et al.*, 2013a and 2013b; Blunt *et al.*, 2013; Li *et al.*, 2015; Han and Liu, 2020; Santos *et al.*, 2020; Tembely *et al.*, 2021). Numerical simulations of petrophysical properties at pore-scale, such as flow and elastic properties, can be divided into two categories: (i) pore-network modeling (PNM) (Dong *et al.*, 2007) and (ii) direct modeling, which encompasses the finite difference method (FDM) (Blunt *et al.*, 2013; Mostaghimi *et al.*, 2013), the finite element method (FEM) (Andrä *et al.*, 2013b), the finite volume method (FVM) (Guibert *et al.*, 2015), the smoothed-particle hydrodynamics method (Pereira *et al.*, 2011), and the lattice Boltzmann method (LBM) (Keehm, 2003; Meng *et al.*, 2008; Andrä *et al.*, 2013a and 2013b; Blunt *et al.*, 2013; Li *et al.*, 2015; Han and Liu, 2020). Among these methods, LBM emerges as the most efficient and accurate approach for both single phase and multiphase flow as it relies on raw images of the rock without any simplification, gridding, or meshing of the pore space (Keehm, 2003). Among the different techniques, the appropriate method can be chosen by balancing between computing time and computational cost. The resource-intensive nature of LBM simulation is depicted in Figure 1, where the computation time increases drastically as the porosity of the rock decreases (Santos *et al.*, 2020).

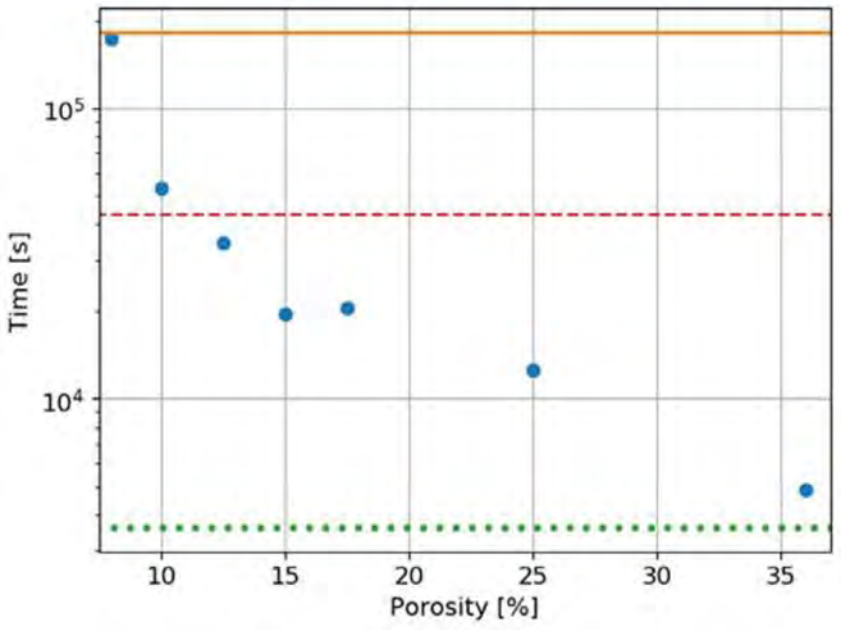

Figure 1—Computational time of LBM simulation vs. porosity of sphere pack samples (Santos *et al.*, 2020).

Recently, machine-learning (ML) has emerged as a computer framework technology that is able to learn from observational data to predict variables of interest (Santos *et al.*, 2020; Sudakov *et al.*, 2019; Tembely *et al.*, 2020a;). The ability of ML algorithms to encode the relationship between many parameters renders

this technology attractive to solve many scientific problems and gain insights from data in an accurate and fast way. The use of ML models has aided in overcoming the computational drawbacks of direct simulations. In recent years, extensive work has been dedicated into training various ML models to predict different petrophysical properties from digital rock images using results from single-phase direct simulation on micro-CT dry images and synthetically generated images.

In this paper, we review the applications of ML algorithms including both shallow- and deep-learning algorithms, taking advantage of the classified categories proposed by Wang *et al.* (2021) and expanding the study with additional research work and deeper critical review. First, the paper discusses the workflow utilized to obtain petrophysical properties from rock images using ML. This is followed by an overview of the key concepts and methods of data acquisition, direct simulation, and ML techniques. Micro-CT imaging, synthetic image generation techniques, mesh-based direct simulation methods, lattice-Boltzmann simulation method (LBM), and various ML algorithms all will be covered. Furthermore, a summary in the form of evaluation metrics along with their mathematical formulations is presented. Finally, a critical literature review is provided, followed by the main findings and conclusions of the study.

Machine Learning Workflow

A typical workflow for predicting rock petrophysical properties from images using direct simulation and machine learning techniques is shown in Figure 2.

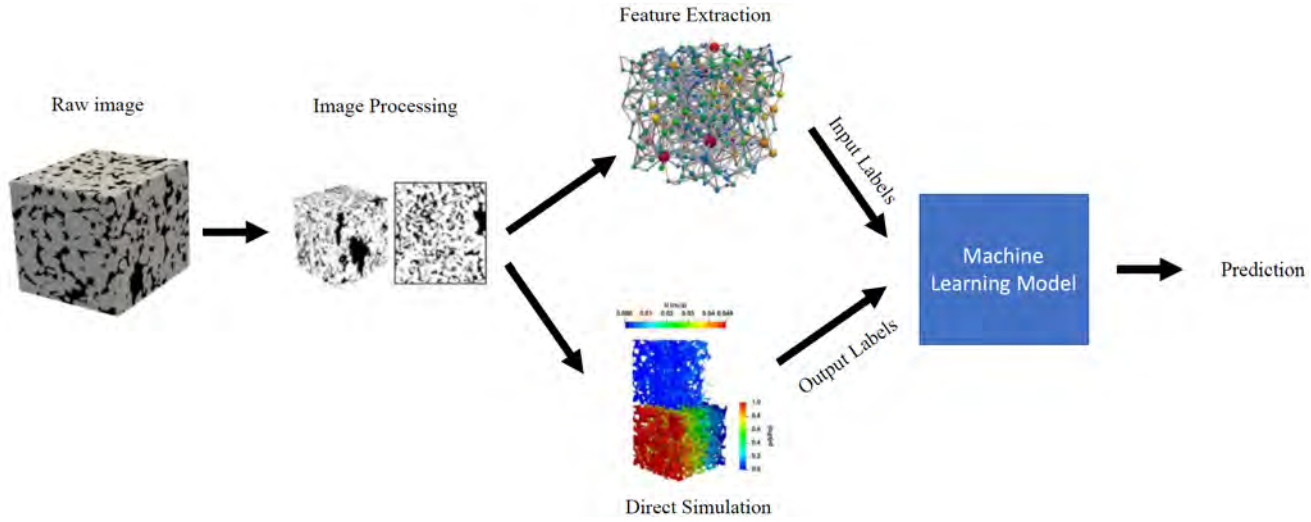

Figure 2—Typical workflow of predicting petrophysical properties using machine learning.

The presented workflow can be used to predict any petrophysical property including porosity, permeability, effective diffusivity (D_e) as well as elastic properties such as young's modulus and shear modulus. Elastic properties are usually computed at pore-scale using the finite element method (FEM). However, applications of ML to predict elastic properties is still to be fully addressed. In the ML context, it is worth noting that the feature extraction step is essential for relating the microscopic properties of porous media extracted from their images to their macroscopic properties, rendering the predictions more interpretable and the ML model more physically informed. Nevertheless, this feature extraction step was not used in all studies and deep learning algorithms were applied instead. Deep learning algorithms deal directly with images to make predictions without any manual intervention.

Image Acquisition and Processing

Digital images are considered the building blocks of all the studies presented in this work. Digital images are made of picture elements called pixels. The size of an image is determined by the dimensions of the pixel matrix. In 3D, these pixels are called voxels. To obtain realistic rock images experimentally, micro-CT imaging technique is usually used. Micro-CT scan is a digital imaging technique that uses X-rays to see inside the object. It captures series of 2D images called slices at different projection angles. Then, a reconstruction process is made from a large number of radiographs to have the 3D image (Andrä *et al.*, 2013a). Micro-CT enables to capture heterogeneities of the core samples at pore-scale including those of carbonates (Menke *et al.*, 2021). In addition, micro-CT scans (typically with a resolution of 0.5μm) exhibits higher resolution than medical-CT (typically with a resolution of 500μm). However, many times these experimental images are not widely available or prohibitively costly to acquire. To circumvent this issue, a variety of synthetic data generation techniques were used to generate porous media structures with specific property ranges (Wu *et al.*, 2012 and 2018; Stenzel *et al.*, 2017; Kamarava *et al.*, 2019; Tian *et al.*, 2020). Furthermore, given their ability to produce structures that are highly correlated to actual images, generative adversarial networks (GANs) have recently been used to generate porous media images (Wang *et al.*, 2021).

Given the high cost and time required for experimental methods, it is obvious that obtaining a large number of images using synthetic imaging techniques is straightforward and was widely adopted in the literature. Work conducted on actual experimental data dealt with this issue by subsampling small number of large images into large number of small images. However, this technique was not clearly explained in most of the literature except for Hong and Liu (2020). This technique, as shown in Figure 3, involves shifting a predetermined window of the size of the desired small image with a certain step size, called the striding distance (Alqahtani *et al.*, 2021), through the original image to obtain small windows if working with 2D images or small cubes in case of 3D images. The size of the images to be trained remains a contentious issue and is often overlooked in most of the studies. Hong and Liu (2020) suggested that the window size be smaller than the representative elementary volume (REV) of the large image in order to obtain a dataset that is widely distributed with a wide range of properties to aid in generalizing the ML model and improving prediction capability.

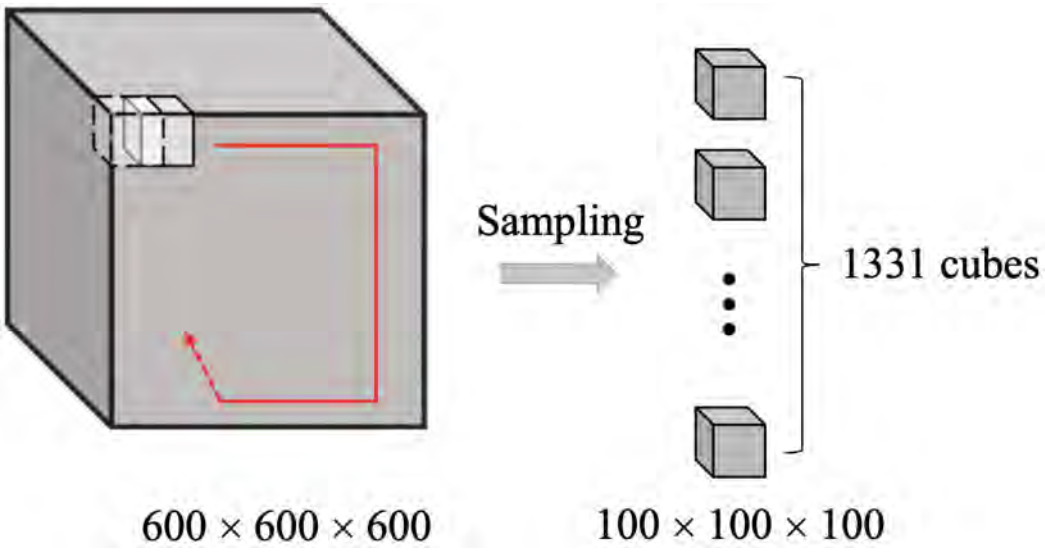

Figure 3—Subsampling of experimental obtained porous media images where the white cube is the sliding window, and the red line is the moving path (Hong and Liu 2020).

Direct Simulation Techniques

To obtain the petrophysical properties data required for training the ML models, direct simulation techniques are used. Direct simulation techniques can be divided into two main categories: discrete particle-based simulation and continuum mesh-based simulation.

Discrete Particle-based Direct Simulation

LBM is the most efficient discrete particle method for simulating fluid flow at the pore-scale. LBM direct simulation is a mesoscopic model based on cellular automata theory and is able to calculate the flow in actual complex porous media without the need of special gridding (Keehm, 2003; Andrä *et al.*, 2013a; Saxena *et al.*, 2017; Graczyk and Matyka, 2020). The fundamental concept of cellular automata theory is that fluids can be considered as combination of large number of small particles moving with random motions. Particles keep colliding and streaming in a billiard-like collision conserving momentum and energy. This process can be simulated by the Boltzmann transport equation as follows (Mohamad, 2019):

$$\frac{\partial f}{\partial r}V+\frac{\partial f}{\partial t}=\Omega, \tag{1}$$

where $f(r,v,t)$ is the particle density distribution function, v is the particle velocity, and Ω is the collision operator. In terms of accuracy, LBM outperforms other direct simulation methods, however, computing time and resources are significant and must be taken into consideration.

Mesh-based Direct Simulation. Mesh-based techniques such as the finite difference method (FDM), finite volume method (FVM), and finite element method (FEM) are used to assess petrophysical properties. The mesh-based approach divides the pore space into geometrically simple cells or elements. For flow properties computation, these techniques are implemented to solve fluid flow equations within the porous media by discretizing the mass and momentum conservation equations:

$$\nabla.v=0, \tag{2}$$

$$\rho v\nabla v=\nabla p+\nabla.(\mu\nabla v), \tag{3}$$

where v represents the velocity vector, ρ is the density, p is the pressure, and μ is the viscosity. The permeability can be calculated using Darcy's law after solving equations (2) and (3). The volume of fluid method (VOF) is an extension of the FVM that can be used to estimate multiphase flow properties for both Newtonian and non-Newtonian fluids (Raeini *et al.*, 2014; Tembely *et al.*, 2020b). While FEM has been used to model flow properties to varying degrees of success. The computation of elastic properties based on rock micro-CT images is one of the most successful application of FEM. The approach consists of discretizing linear elastic equation of Hooke's law (Garboczi and Kushch, 2015):

$$\sigma=C\varepsilon, \tag{4}$$

where σ represents the stress tensor, C is the stiffness tensor, and ε is the strain tensor. By solving equation (4) on the 3D micro-CT image with homogeneous strains, the effective bulk (K) and shear moduli (G) can be computed (Garboczi and Kushch, 2015; Jouini and Vega, 2011).

Machine Learning Techniques

Machine-learning (ML) involves algorithms that extract information from data, process it to facilitate tasks automation, and enhance human knowledge about the subject under examination. There are three types of learning algorithms, as shown in Figure 4: supervised, unsupervised, and semi-supervised learning (Brunton *et al.*, 2020). This subdivision is based on the degree to which the available data is labeled. Supervised learning is employed with labeled data, in which the input and output of the problem are known in advance, and the learning algorithm is asked to encode the relationship between them to help in future predictions. On the other hand, unsupervised learning algorithms work with unlabeled data, which means that the input data

is known but the output is not known, and the ML model is used to extract patterns and information from the data. Classification and regression algorithms are examples of supervised learning, whereas clustering and dimensionality reduction algorithms are instances of unsupervised learning. Meanwhile, semi-supervised learning deals with partially labeled data (a small amount of labeled data with large amount of unlabeled data) and includes algorithms such as generative adversarial networks (GAN) and reinforcement learning (RL) (Brunton *et al.*, 2020; Santos *et al.*, 2020).

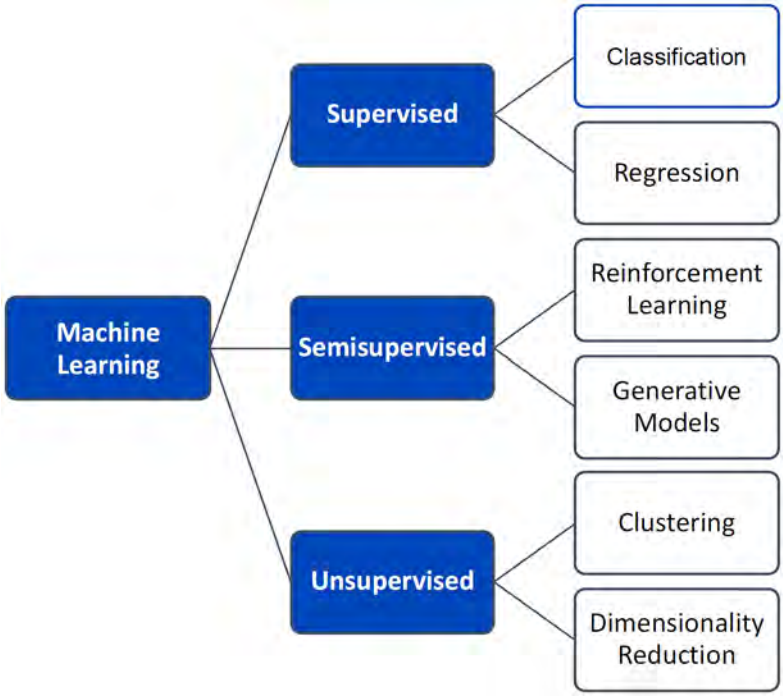

Figure 4—Classification of ML algorithms.

Commonly used regression algorithms include tree-based algorithms and artificial neural networks (ANNs). Tree-based algorithms include decision trees and their powerful ensembles such as random forests, gradient boosting and gradient xboosting. On the other hand, ANNs, as shown in Figure 5, have the power to encode and approximate any non-linear function. Improvements in ANNs are deep neural networks (DNNs) and convolutional neural networks (CNNs). DNNs are neural networks with many layers which can offer impressive predictive capabilities even with the most complex data while CNNs are DNNs with non-linear activation functions expressed as convolution kernels giving them high performance in image recognition and analysis (LeCun *et al.*, 2015; Brunton *et al.*, 2020).

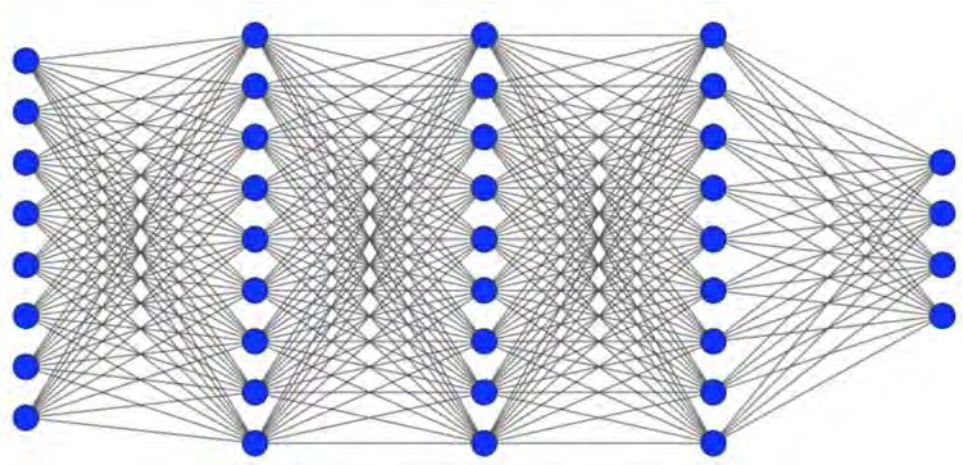

Figure 5—Schematic of an ANN with three hidden layers.

Regression Evaluation Metrics

This section defines different evaluation metrics that are used to evaluate the performance of ML models. If y_i is the original output, $\hat{y}_i$ is the predicted output by the model, and $\bar{y}$ is the original outputs mean, the evaluation metrics can be defined as shown in Table 1.

Table 1—ML-Models Evaluation Metrics

Metric	Definition	Mathematical Definition	Optimal value
Absolute Error	Absolute error is the absolute value of the difference between the actual output and the predicted output.	$AE = \lvert y_i - \hat{y}_i \rvert$	0
Relative Error	Relative error is defined as the absolute error divided by the original output value.	$RE = \frac{\lvert y_i - \hat{y}_i \rvert}{y_i}$	0
Mean-Squared Error	Mean-squared error is the average of the absolute error squares for all the data points.	$MSE = \frac{1}{n}\sum_{i=1}^{n}(y_i - \hat{y}_i)^2$ where n is the number of data points.	0
Truncated Relative Error	Truncated relative error is different from relative error where it does not relate the absolute error to the original output; instead, it relates absolute error to a pre-specified threshold value.	$TRE = \frac{\lvert y_i - \hat{y}_i \rvert}{y^{thsd}}$ where y^{thsd} is a pre-defined threshold value of the output.	0
Coefficient of Determination (R^2)	Coefficient of determination, usually called R^2, is used to test how good the regression model fits the actual data.	$R^2 = 1 - \frac{SS_{res}}{SS_{tot}}$ $SS_{tot} = \sum_{i=1}^{n}(\hat{y}_i - \bar{y})^2$ $SS_{res} = \sum_{i=1}^{n}(y_i - \bar{y})^2$	1

Predicting Petrophysical Properties Using Machine Learning

The approaches to predict petrophysical properties from images using ML can be categorized into two main classes. The first class is a regression model, which uses image features or the images themselves to train the

model in order to encode their relationship with the relevant petrophysical property of interest. The second class employs ML as a proxy model for numerical simulation, with the ML model capable of predicting the velocity field, which in turn can be used to recover the physical properties of interest. Both classes along with their subcategories are presented in Figure 6, which will be discussed in the sections below.

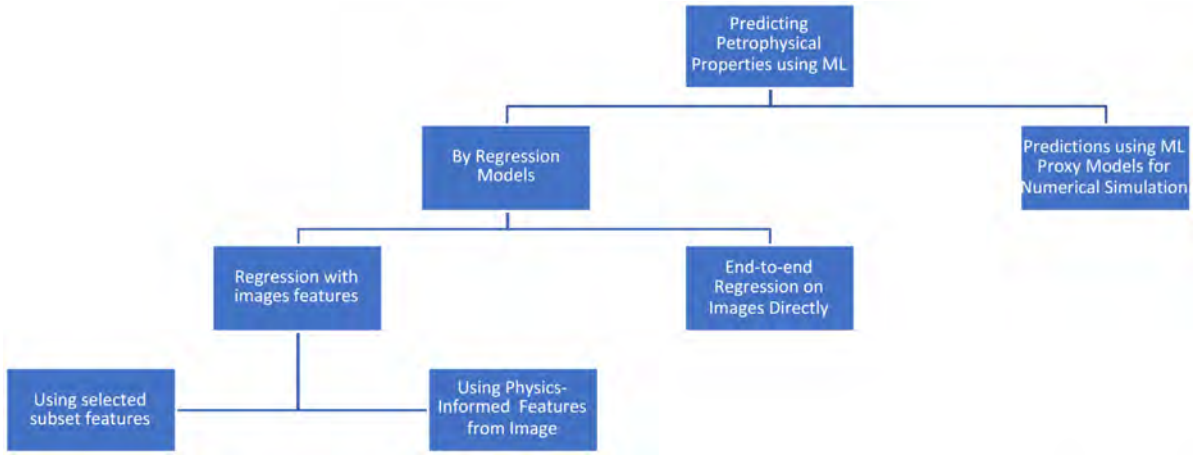

Figure 6—Classification of different ML approaches used to estimate petrophysical properties from images.

Predictions by Regression Models

A relationship between a petrophysical property and the porous media structure can be established using the conventional ML techniques, which requires simplifying the porous structure into some descriptors or features that can be correlated to the petrophysical property using conventional regression models. This technique is typically recommended in the literature since it reveals the physical knowledge about the problem and has a low computational cost. The other method involves the use of deep learning (DL) techniques which mainly uses images of the rocks as direct input, so features from the images do not need to be extracted first. This technique, despite being somewhat computationally expensive and needs optimization of many hyperparameters of the ANNs, it does not involve any human intervention. Both techniques are presented below with critical analysis of related case studies from the literature.

Regression with Images Features. In regression with image features, porous media is statistically characterized using different morphological features. These features can be extracted from the images of the porous media using pore network models. However, all the features cannot be related to all the petrophysical properties of the porous media. Some features affect permeability; others affect effective diffusivity, and so on. In addition, the inclusion of irrelevant features in the model makes the model more complex and harder to interpret. The selection of features can be correlated to a specific petrophysical property, one should usually refer to the known empirical correlations or the experimental results. This method of feature selection was employed in most of the studies discussed in this paper. On the other hand, some studies have used feature-selection algorithms, which assign a score to the feature based on the extent the feature is correlated to the investigated petrophysical property.

Regression Using Selected Subset Features. Permeability estimation from images was among the first applications of ML regression models in porous media research (Van der Linden *et al.*, 2016). In the latter study, permeability was characterized through feature selection with the highest score features that can predict permeability accurately. For establishing a linear correlation in log-log scale between permeability and average closeness centrality of weighted pore network as a feature, three ML feature selection techniques were used—Kendall rank correlation, mutual information, and RReliefF. The latter techniques give a score to image features depending on the degree of optimally characterizing permeability.

The dataset comprised 536 sphere packings that were generated using the discrete element method (DEM), and features were extracted using a pore network and a particle contact network.

Furthermore, Yasuda *et al.* (2021) extended the latter work and developed a workflow that not only ranks the features according to their effects on permeability calculation, but also is able to chooses the best subset of features to accurately describe the permeability.

Regression Using Physics-informed Features of Images. Studies in this category, first, extracted some features from the images that were known to affect the investigated petrophysical property. Rabbani and Babaei (2019) estimated pore-scale permeability by coupling both direct and indirect methods; the combination of PNM with LBM to benefit from strengths of both approaches. Pore network extraction was implemented using watershed segmentation algorithm on twelve 3D porous rock images. Moreover, Tian *et al.* (2020) proposed a hybrid ML method to implicitly build a nonlinear relationship between permeability and pore structure parameters, such as tortuosity, number of pores, and pore-throat ratio, to overcome the challenges in permeability predictions due to the complicated pore structure of the rocks.

In addition, Tembely *et al.* (2020a) extracted porosity, PNM permeability, and formation factors then tested various algorithms to predict absolute permeability from carbonate-rock images. The study alongside with CNNs and physics informed CNNs, used random forest, gradient boosting and gradient xboosting. Furthermore, Röding *et al.* (2020) extracted other features such as two- and three-point correlation function, geodesic tortuosity, porosity, and specific surface area. The authors found that the combination of all the three two-point correlation functions with geodesic tortuosity resulted in the best performance of the model. Table 2 presents a summary between studies of different ML regression with image-features form the literature trained on direct simulation data for permeability estimation from rock images.

Table 2—Comparison between studies of different ML regression with image-features trained on direct simulation data to get permeability from porous media images

No.	Author	Model	Predicted parameter	Training Set	Extracted features	Algorithm	Accuracy
1	Van der Linden *et al.*, (2016)	3D	Permeability	536 artificially generated samples of porous, granular media using DEM (discrete element methods) and a reference case of a real sphere packing	27 features most significant one was pore network closeness centrality	Linear regression	RMSE = 0.17 and R^2 = 0.98
2	Yasuda *et al.* (2021)	3D	Permeability	528 synthetically generated porous structures of size 320×240×240 voxels	154 structure descriptors	Support vector machine (SVM)	–
3	Rabbani and Babaei (2019)	2D pore throat images	Permeability of pore throats	9333 2D cross sections of throats extracted using PNM	7 morphological parameters – Cross-section area – Wetted perimeter – Axes ratio – Equivalent diameter – Solidity – Hydraulic radius – Mean Distance	1- ANN (trained on all 7 features) 2- ANN (trained on only Mean distance)	R^2 = 0.9996, MSE = 0.0264 2- R^2 = 0.9982, MSE = 0.1971
4	Tian *et al.* (2020)	3D	Permeability	1000 3D synthetic samples of size 100×100×100	16 geometric measures including: – Tortuosity – No. of pores – Pore-throat ratio	Hyprid GA-ANN algorithm with: – 9 layers – 1 dense layer – (74-195) neurons	R^2 = 0.999
5	Tembely *et al.* (2020a)	3D	Permeability	3D carbonate micro-CT images	• Porosity • PNM Permeability	• Gradient Boost • Random Forest	R^2 for each algorithm:

No.	Author	Model	Predicted parameter	Training Set	Extracted features	Algorithm	Accuracy
					• Formation Factor	• Gradient XBoosting DNN •CNN	• 0.88 • 0.90 • 0.91 • 0.916 • 0.913 •
6	Röding *et al.*(2020)	2D	Permeability	30000 virtual microstructures of different types including both granular and continuous solid phases	• One-point correlation functions: porosity, specific surface • two-point correlation functions: surface-surface, surface-void and void-void correlations functions • geodesic tortuosity	CNN	MSE = 0.026

End-to-end Regression on Images Directly. The direct prediction of permeability in a robust way from images using CNNs is a novel pore-scale modeling method that showed a great potential in the study of Wu *et al.* (2018). The predicted permeabilities for most samples had less than 10% error compared to the LBM simulation results. However, the accuracy of the model increased by injecting the porosity and specific area of the image in a physics-informed CNN. Moreover, in a different study that included 3D sandstone images, hundreds of their stochastic realizations generated by a reconstruction method, and synthetic unconsolidated porous media produced by a Boolean method, a hybrid network of ANN and DL was developed to predict permeability (Kamrava *et al.*, 2019).

Wu *et al.* (2019) performed a study to predict the effective diffusivity (D_e) of 2D porous media. AlexNet was tested along with ResNet50. A reconstruction method was implemented to generate porous media varying in pore topology and porosity, and LBM was used to compute the effective diffusivity that was recovered by Fick's law. The models were more robust six orders of magnitude of computation cost than LBM simulations. A truncated error of less than 10% was reported for 95% of the samples with D_e larger than 0.2.

In another study, Araya-Polo *et al.* (2020) subsampled and cropped a high-resolution image of size 33020 × 9434 to patches to match the GPU memory, resulting in a couple of hundred of 640 × 480 images. Two neural networks were built where the first one was composed of seven convolutional layers and two dense layers while the second one had a structure like the U-net. The networks showed high accuracy with R^2 of 0.9582 and MSE of 0.0108. Additionally, Graczyk and Matyka (2020) used a similar workflow to obtain porosity, permeability, and tortuosity from synthetic images. The dataset in this project is considered the largest ever used among other studies with 84917 and 14986 samples in training and validation, respectively.

For CNN to learn from greyscale images as has been done with binary/segmented images in the literature, Alqahtani *et al.* (2020) developed a workflow to rapidly estimate the porosity, specific surface area and average pore size of porous media using CNNs. Furthermore, Alqahtani *et al.* (2021) applied ResNet and ResNext; two convolutional neural network architectures, to learn the geometry of the pore space in 3D porous media images. This study had one of the highest number of dataset images accounting for more than 29K virtual geometries with a wide range of permeabilities extending over more than 3 orders of magnitude. The permeability of the images to train the models was computed using pore-scale finite volume solver.

However, the above analysis concentrated on evaluating the mean overall permeability of the samples, but permeability in most cases is an anisotropic property, i.e., its value changes depending on the direction of evaluation. Hong and Liu (2020) proposed a 3D CNN-based approach for rapidly estimating permeability

in anisotropic rock. The workflow showed high R^2 scores as well as good generalization ability in predicting the permeability of other samples. The method was 10,000 times faster than LBM in permeability prediction. Table 3 presents a summary of different ML regression with image directly studies form the literature trained on direct simulation data for permeability estimation from rock images.

Table 3—Comparison between different ML end-to-end regression with images directly studies from the literature trained on direct simulation data to get petrophysical properties from porous media images.

No.	Author	Model	Predicted parameter	Training Set	Algorithm	Accuracy
1	Wu *et al.* (2018)	2D	Permeability	Voroni Mesh-based geometries with throats Deviates from Kozeny-Carmen equation	• CNN • Physics-informed CNN	R^2 for each algorithm: • 0.878642 • 0.926315
2	Kamrava *et al.* (2019)	3D	Permeability	500 stochastically generated samples of size 200^3	DL-ANN hyprid network	$R^2 = 0.91$
3	Wu *et al.* (2019)	2D	Effective Diffusivity	2D porous material generated using quartet structure generation set (QSGS) method	•Regular CNN • Porosity- informed CNN • CNN with preprocessed image	Mean TRE for each algorithm: • (41.7-86.8)% • 59.2% • 29.7%
4	Araya-Polo *et al.* (2019)	2D	Permeability	2D colored sandstone images from 11 clastic reservoirs across Shell's asset portfolio and 135 different cores	DNN	Average MSE of predictions is 11.69% for k in the range of 50-1100 mD
5	Graczyk and Matyka (2020)	2D	Porosity • Permeability • Tortuosity	100,000 binary pictures of size 800×400 prepared using random deposition model of porous media. The input to the network is of size 400 × 400	CNN	• Best accuracy for porosity.
6	Alqahtani *et al.* (2020)	2D	• Porosity • Specific surface area • Average pore size	7262 sub-images of three different sandstone tomograms	5 layers CNN + one dense layer	• Porosity: $R^2 = 0.96$, MRE < 3% for binary images MRE = 6.3% for grayscale images • Specific surface area $R^2 = 0.92$, MRE = 3.9% $R^2 = 0.79$, MRE = 5.8% • Average pore size MRE=6% MRE=6.7%
7	Hong and Liu (2020)	3D	• K_x • K_{yz} • K_{mean}	1331 small cubes of coconino sandstone etended to 3158 by shrinking and expanding algorithm	3D CNN with: – convolutional layers: to extract features – pooling layers: to reduce the no. of features – fully connected layers: to do classification	R^2 for each permeability • K_x: $R^2 = 0.8972$ • K_y: $R^2 = 0.8821$ • K_z: $R^2 = 0.8201$
8	Alqahtani *et al.* (2021)	2D	• Porosity • Coordination number • Average pore size	7860 images (128×128) split into 5680 for training and 2000 for testing	CNN (5 convolution layers + 2 dense layers)	Average error 5%, 20%, 7%

Predictions by ML Proxy Models for Numerical Simulation. In this section, another approach to predict petrophysical properties of porous rock using ML as a proxy model for numerical simulation is discussed. This approach involves replacing the high-cost direct simulation methods with ML methods and then using the resulting velocity field to calculate the desired petrophysical property of the rock. The use of

ML in simulation has been reported in different studies (Wang *et al.*, 2021). Some studies were able to replace the simulation with reasonable accuracy; however, other studies suggested that with the obtained accuracy, simulation could not be replaced but can be improved by using the resulting velocity field as an initial condition, allowing the simulation to converge quickly. Table 4 compares the studies used to predict petrophysical properties from velocity fields derived using trained ML algorithms, including the works of Santos *et al.* (2020), Wang *et al.* (2020) and Santos *et al.* (2021). The three studies developed three distinct neural network architectures known as PoreFlow-Net, ML-LBM and MS-Net, respectively.

Table 4—Comparison between different prediction studies using ML proxy models for numerical

No.	Author	Model	Predicted parameter	Training Set	Extracted features	Algorithm	Testing Set (if different from training)	Accuracy
1	Santos *et al.* (2020)	3D	Permeability	4 sphere packs	•Euclidean Distance • Max. Inscribed Sphere • Time of Flight	CNN (PoreFlow-Net)	• Fontainebleau sandstone • Eroded Sphere Pack • Estaillades limestone • Microsand • Castlegate sandstone • Bentheimer sandstone	RE for each of the testing sets: • (1.44-24)% • 23.53% 5.45% • 17.01% • 1.06% • 27.30%
2	Wang *et al.* (2020)	2D and 3D	Permeability	• 10,000 2D structure generated stochastically of size 256 × 256 and a correlation length in range (8: 64) • 1,000 3D images of size 128^3	• Roughness • Contact angle	CNN (Ml-lbm)	–	RE=1.0801%
3	Santos *et al.* (2021)	3D	Permeability	Five numerically dilated sphere packs of size (265 × 265 × 265) voxels	Euclidean Distance	CNN (MS-Net)	Fontainebleau sandstone • Artificially created samples • Realistic samples • Fractured domains	RE for each of the testing sets: • (0.87-1.13)% • (0.83-0.94)% • (1.08-1.39)% • (0.20-0.95)%

Summary and Conclusions

After the review of techniques to determine rock petrophysical properties from porous media images, the following conclusions can be drawn:

- Estimating petrophysical properties of rocks is crucial, and several methods have been developed over the past decades to perform this task, ranging from experimental methods, empirical correlations to direct simulation techniques.
- Each of these methods has drawbacks, including long computational time and the capability to generalize well for predicting unseen dataset. As a result, machine-learning (ML), which provides different algorithms that can encode the most complex nonlinear relationships between variables, is proposed to be used to assist in the task of petrophysical properties estimation and overcome the cost and time limitations of the aforementioned methods.
- The workflow of estimating petrophysical properties from porous media images using direct simulation techniques and ML algorithms was presented. The steps common to all the workflows were discussed with examples from the literature. Subsequently, a comprehensive review of recent studies was analyzed and compared in terms of dataset and model accuracy. A general framework

summarizing all the studies was provided. Furthermore, a contrast in assessing the petrophysical properties from the different studies was highlighted.

- Some studies used direct regression between either the features extracted from the image or the images themselves and the corresponding petrophysical property of interest. On the other hand, other studies preferred to use ML as an alternative to simulation, where ML models can be trained to predict the simulation properties field (velocity and pressure), enabling the calculations of the petrophysical properties of interest.
- Although the models that used images directly were developed to eliminate any human intervention, they were significantly improved when incorporated with physical-based features shifting the ML model to be physics-informed.

Acknowledgements

The authors wish to acknowledge Abu Dhabi National Oil Company (ADNOC) for funding this research and Khalifa University of Science and Technology for the support and encouragement.

Nomenclature Symbols

K	Bulk moduli
R^2	Coefficient of determination
Ω	Collision operator
ρ	Density
D_e	Effective diffusivity
n	Number of data set
y_i	Original output
$\bar{y}$	Original outputs mean
y^{thsd}	Output threshold value
f	Particle density distribution function
r	Particle location
v	Particle velocity
$\hat{y}_i$	Predicted output
p	Pressure
S_{or}	Residual oil saturation
ss_{res}	Residual sum of squares
G	Shear moduli
C	Stiffness tensor
ε	Strain tensor
σ	Stress tensor
t	Time
ss_{tot}	Total sum of squares
μ	Viscosity

Abbreviations

AE	Absolute Error
ANN	Artificial Neural Network
CNN	Convolutional Neural Network
CT	Computed Tomography
DNN	Deep Neural Network
FDM	Finite-Difference Method

FEM	Finite Element Method
FVM	Finite Volume Method
GAN	Generative Adversarial Network
LBM	Lattice-Boltzmann Method
ML	Machine Learning
MSE	Mean-Squared Error
PNM	Pore-Network Model
QSGS	Quartet Structure Generation Set Method
RE	Relative Error
REV	Representative Elementary Volume
RL	Reinforcement Learning
SVM	Support Vector Machine
TRE	Truncated Relative Error

References

Alqahtani, N., Alzubaidi, F., Armstrong, R. T., Swietojanski, P., and Mostaghimi, P., 2020. Machine Learning for Predicting Properties of Porous Media from 2d X-ray Images. *Journal of Petroleum Science and Engineering*, **184**: 106514.

Alqahtani, N., Chung, T., Wang, Y. D., Armstrong, R. T., Swietojanski, P., and Mostaghimi, P., 2021. Flow-Based Characterization of Digital Rock Images Using Deep Learning. *SPE Journal*, **26**(4): 1800–1811.

Andrä, H., Combaret, N., Dvorkin, J., Glatt, E., Han, J., Kabel, M., Keehm, Y., Krzikalla, F., Lee, M., Madonna, C., Marsh, M., Mukerji, T., Saenger, E. H., Sain, R., Saxena, N., Ricker, S., Wiegmann, A., and Zhan, X., 2013a. Digital rock physics benchmarks—Part I: Imaging and segmentation. *Computers and Geosciences*, **50**(1): 25–32.

Andrä, H., Combaret, N., Dvorkin, J., Glatt, E., Han, J., Kabel, M., Keehm, Y., Krzikalla, F., Lee, M., Madonna, C., Marsh, M., Mukerji, T., Saenger, E. H., Sain, R., Saxena, N., Ricker, S., Wiegmann, A., and Zhan, X., 2013b. Digital rock physics benchmarks—part II: Computing effective properties. *Computers and Geosciences*, **50**(1): 33–43.

Araya-Polo, M., Alpak, F. O., Hunter, S., Hofmann, R., and Saxena, N., 2019. Deep learning–driven permeability estimation from 2D images. *Computational Geosciences*, **24**(2): 571–580.

Blunt, M. J., Bijeljic, B., Dong, H., Gharbi, O., Iglauer, S., Mostaghimi, P., Paluszny, A., and Pentland, C., 2013. Pore-scale imaging and modelling. *Advances in Water Resources* **51**: 197–216.

Brunton, S. L., Noack, B. R., and Koumoutsakos, P., 2020. Machine Learning for Fluid Mechanics. *Annual Review of Fluid Mechanics*, **52**(1): 477–508.

Dong, H., Touati, M., and Blunt, M. J., 2007. Pore Network Modeling: Analysis of Pore Size Distribution of Arabian Core Samples. Paper SPE 105156, SPE Middle East Oil and Gas Show and Conference, Manama, Bahrain.

Garboczi, E. J. and Kushch, V. I., 2015. Computing elastic moduli on 3-D X-ray computed tomography image stacks. *Journal of the Mechanics and Physics of Solids*, **76**: 84–97.

Graczyk, K. M. and Matyka, M., 2020. Predicting porosity, permeability, and tortuosity of porous media from images by deep learning. *Scientific Reports*, **10**(1): 21488.

Guibert, R., Nazarova, M., Horgue, P., Hamon, G., Creux, P., and Debenest, G., 2015. Computational Permeability Determination from Pore-Scale Imaging: Sample Size, Mesh and Method Sensitivities. *Transport in Porous Media*, **107**: 641–656

Hong, J. and Liu, J., 2020. Rapid estimation of permeability from digital rock using 3d convolutional neural network. *Computers and Geosciences*, **24**(5): 1523–1539.

Jouini, M. S., and Vega, S., 2011. Simulation of elastic properties in carbonates. *Leading Edge*, **30**(12): 1400–1407.

Kamrava, S., Tahmasebi, P., and Sahimi, M., 2019. Linking morphology of porous media to their macroscopic permeability by deep learning. *Transport in Porous Media*, **131**: 427–448.

Keehm, Y., 2003. Computational rock physics: Transport properties in porous media and applications. *Ph.Dissertation D.*, Stanford University, California, USA.

LeCun, Y., Bengio, Y., and Hinton, G., 2015. Deep Learning. *Nature*, **521**: 36–444.

Li, H., Yang, W., Huang, H., Chevalier, S., Sassi, M., Zhang, T., Zahaf, K., and Al-Farisi, O., 2015. Pore-Scale Lattice Boltzmann Simulation of Oil-Water Flow in Carbonate Rock with Variable Wettability. Paper SPE 177548, Abu Dhabi International Petroleum Exhibition and Conference, Abu Dhabi, UAE.

Meng, J., Qian, Y., Li, X., and Dai, S., 2008. Lattice Boltzmann model for traffic flow. *Physical Review E*, **77**(3): 036108.

Menke, H. P., Maes, J., and Geiger, S., 2021. Upscaling the porosity–permeability relationship of a microporous carbonate for Darcy-scale flow with machine learning. *Scientific Reports*, **11**: 2625.

Mohamad, A., 2019. Lattice Boltzmann Method Fundamentals and Engineering Applications with Computer Codes. Springer, 2nd Edition, London, UK.

Mostaghimi, P., Blunt, M.J. and Bijeljic, B., 2013. Computations of Absolute Permeability on Micro-CT Images. *Mathematical Geosciences*, **45**: 103–125.

Pereira, G. G., Prakash, M., and Cleary, P. W., 2011. SPH modelling of fluid at the grain level in a porous medium. *Applied Mathematical Modelling*, **35**(4), 1666–1675.

Rabbani, A. and Babaei, M., 2019. Hybrid pore-network and lattice-boltzmann permeability modelling accelerated by machine learning. *Advances in Water Resources*, **126**: 116–128.

Raeini, A. Q., Blunt, M. J., and Bijeljic, B., 2014. Direct simulations of two-phase flow on micro-CT images of porous media and upscaling of pore-scale forces. *Advances in Water Resources*, **74**: 116–126.

Röding, M., Ma, Z., and Torquato, S., 2020. Predicting Permeability via Statistical Learning on Higher-order Microstructural Information. *Scientific Reports*, **10**: 15239.

Santos, J. E., Xu, D., Jo, H., Landry, C. J., Prodanović, M., and Pyrcz, M. J., 2020. PoreFlow-Net: A 3D convolutional neural network to predict fluid flow through porous media. *Advances in Water Resources*, **138**: 103539.

Santos, J. E., Yin, Y., Jo, H., Pan, W., Kang, Q., Viswanathan, H., Prodanović, M., Pyrcz, M., and Lubbers, N., 2021. Computationally efficient multiscale neural networks applied to fluid flow in complex 3D porous media. Transport in porous media: 1573-1634.

Saxena, N., Mavko, G., Hofmann, R., and Srisutthiyakorn, N., 2017. Estimating permeability from thin sections without reconstruction: Digital rock study of 3D properties from 2D images. *Computers and Geosciences*, **102**: 79–99.

Stenzel, O., Pecho, O., Holzer, L., Neumann, M., and Schmidt, V., 2017. Big Data for Microstructure-Property Relationships: A Case Study of Predicting Effective Conductivities. *AIChE Journal*, **63**(9): 4224–4232.

Sudakov, O., Burnaev, E., and Koroteev, D., 2019. Driving digital rock towards machine learning: Predicting permeability with gradient boosting and deep neural networks. *Computers and Geosciences*, **127**: 91–98.

Tembely, M., Alameri, W. S., AlSumaiti, A. M., and Jouini, M. S., 2020b. Pore-Scale Modeling of the Effect of Wettability on Two-Phase Flow Properties for Newtonian and Non-Newtonian Fluids. *Polymers*, **12**: 2832.

Tembely, M., AlSumaiti, A. M., and Alameri, W., 2020a. A deep learning perspective on predicting permeability in porous media from network modeling to direct simulation. *Computational Geosciences*, **24**(4): 1541–1556.

Tembely, M., AlSumaiti, A. M., and Alameri, W., 2021. Machine and deep learning for estimating the permeability of complex carbonate rock from X-ray micro-computed tomography. *Energy Reports*, **7**: 1460–1472.

Tian, J., Qi, C., Sun, Y., Yaseen, Z., and Pham, B., 2020. Permeability prediction of porous media using a combination of computational fluid dynamics and hybrid machine learning methods. *Engineering with Computers*, **3**.

Van der Linden, J., Narsilio, G., and Tordesillas, A., 2016. Machine learning framework for analysis of transport through complex networks in porous, granular media: A focus on permeability. *Physics Review E*, **94**: 22904.

Wang, Y. D., Blunt, M. J., Armstrong, R. T., and Mostaghimi, P., 2021. Deep learning in pore scale imaging and modeling. *Earth-Science Reviews*, **215**: 103555.

Wang, Y. D., Chung, T., Armstrong, R. T., and Mostaghimi, P., 2020. Ml-lbm: Machine Learning Aided Flow Simulation in Porous Media. ArXiv.

Wu, M., Xiao, F., Johnson-Paben, R. M., Retterer, S. T., Yin, X., and Neeves, K. B., 2012. Single- and Two-phase Flow in Microfluidic Porous Media Analogs Based on Voronoi Tessellation. *Lab Chip*, **12**: 253–61.

Wu, H., Fang, W., Kang, Q., Tao, W., and Qiao, R., 2019. Predicting Effective Diffusivity of Porous Media from Images by Deep Learning. *Scientific Reports*, **9**(1): 20387.

Wu, J., Yin, X., and Xiao, H., 2018. Seeing permeability from images: fast prediction with convolutional neural networks. *Science Bulletin*, **63**(18): 1215–1222.

Yasuda, T., Ookawara, S., Yoshikawa, S., and Matsumoto, H., 2021. Machine learning and data-driven characterization framework for porous materials: Permeability prediction and channeling defect detection. *Chemical Engineering Journal*, **420**: 130069.